International Journal of Innovative
Computing, Information and Control
Volume **9**, Number **1**, January **2013**

 ISSN 1349-4198
pp. 81–97

SPECIFIED STRUCTURE MIXED H_2/H_∞ CONTROL-BASED ROBUST FREQUENCY STABILIZATION IN A SMART GRID BY PLUG-IN HYBRID ELECTRIC VEHICLES

Issarachai Ngamroo

School of Electrical Engineering
Faculty of Engineering
King Mongkut's Institute of Technology Ladkrabang
Chalongkrung Rd., Ladkrabang, Bangkok 10520, Thailand
knissara@kmitl.ac.th

Received October 2011; revised February 2012

Abstract. *In the future smart grid, the penetration of wind power tends to increase significantly. This may cause the tie-line power and frequency fluctuations in the power grid. On the other hand, the plug-in hybrid electric vehicles (PHEV) are highly expected to be installed in the customer side. The bidirectional power control of PHEV can be applied to stabilize the power and frequency fluctuations. This paper proposes the specified structure mixed H_2/H_∞ control design of bidirectional power controller of PHEV for robust frequency stabilization of the smart grid with large wind farms. System uncertainties are represented by the multiplicative perturbation model. The structure of power controller is specified as a proportional integral (PI) with single input. The PI parameters optimization problem is formulated based on the enhancement of control performance and robustness against system uncertainties. Without the difficulty of weighting functions selection as in a mixed H_2/H_∞ control, the PI parameters are automatically tuned by particle swarm optimization. Simulation results confirm that the proposed robust controller is much superior to the conventional controller in terms of control performance and robustness against various uncertainties.*

Keywords: Mixed H_2/H_∞ control, Robust control, System uncertainties, Smart grid, Load-frequency control, Particle swarm optimization, Plug-in hybrid electric vehicles

1. **Introduction.** With the large requirement of the reduction of greenhouse gas emission and the environmental friendly energy sources, the smart gird concept has been paid attention around the world [1,2]. A smart grid is the electric power system which integrates the multidisciplinary technology such as power engineering, information, communication control and instrumentation. A smart grid not only enables active participation by consumers in demand response, but also provides high power quality to the customers. Besides, the penetration of renewable energy sources to the smart grid, particularly, the wind power generation tends to increase significantly, because of low impact to environment and infinite availability. Nevertheless, the intermittent power generation from wind energy may cause a large frequency fluctuation problem, especially when the capacity of generators used for frequency control is inadequate. Without effective control, the severe frequency fluctuation may result in the system instability [3].

On the other hand, the plug-in hybrid electric vehicles (PHEV) are significantly expected to be installed in the customer side. With sufficient energy stored in the battery of PHEV, the bidirectional charging and discharging power control of PHEVs or the vehicle to grid (V2G) concept can be applied to alleviate the power fluctuation [4-8]. In [4,5], the power charging control of PHEV has been proposed to control frequency in

an interconnected power system with wind farm. The charging controller is based on a proportional control. Nevertheless, the controllers in [4,5] are able to stabilize the system frequency during charging period only. In other words, when the power generation is greater than the power demand, the PHEV power controller can absorb the surplus power. On the other hand, when the power generation is less than the power demand, the power controller cannot control the system frequency. This is the weak point of the proposed controllers in [4,5]. The ability of bidirectional power control of PHEV whenever the unbalance between power generation and power demand occurs, is high expected. In [6-8], the bidirectional power control or vehicle to grid (V2G) of PHEV has been proposed for frequency control in interconnected power systems with wind farms. The proportional-based PHEV power controller in [6-8] provides satisfactorily control effect. However, the design technique of controller parameters has not been clearly explained. Besides, under various system uncertainties such as variation of system parameters, various wind generations and loads, the PHEV power controller in [6-8] may not tolerate such uncertainties and fail to handle the system frequency fluctuation. The robustness of the controller against system uncertainties is a vital factor which must be taken into account.

To improve the robustness of the controller against system uncertainties, recently, many research works based on H_∞ control have been proposed. In [9], the H_∞ robust controller design of media advance systems with time domain specification has been presented. The network-based H_∞ control of systems with time-varying sampling period has been proposed. From these researches, an H_∞ control is useful for holding close loop stability and formulation of some uncertainties and practical control constraints. Nevertheless, in many real world applications, multi-objectives such as stability, disturbance attenuation and reference tracking under model uncertainties and practical constraints are followed simultaneously. Only the H_∞ control may fail to capture some design specifications such as noise attenuation or regulation against random disturbances. To handle such design specifications, H_2 control can be applied. In [10], the robust H_2 output feedback control has been proposed for a class of time-delay systems. In [11], the derivative state constrained optimal H_2 control has been applied for unstable systems. It can be mentioned that H_∞ or H_2 control is mainly useful to capture a set of individual design specifications.

To deal with the multi-objectives design including all design specifications mentioned above, the combination of H_2 and H_∞ (mixed H_2/H_∞) control has been proposed [12,13]. Besides, the mixed H_2/H_∞ control has been applied to many control systems. In [14], the synthesis of a logic-based switching H_2/H_∞ controller with an intelligent supervisor approach has been proposed. The H_2 and H_∞filtering has been applied to linear systems with unknown inputs and polytopic uncertainty. In [15], the robust automatic voltage regulator design based on mixed H_2/H_∞ pole placement using linear matrix inequality has been presented. Nevertheless, the inevitable problems in the mixed H_2/H_∞ control are the difficulties in selection of weighting functions and the resulted high-order controller [16-18]. In practice, the controller structures such as PI, are preferred because of their simple structure and low order.

To overcome above problems, the specified structure mixed H_2/H_∞ control design of PHEV power controller for robust frequency stabilization in the smart grid with large wind farms is presented in this paper. The multiplicative perturbation model is used to represent unstructured system uncertainties such as variation of system parameters, various loadings and wind patterns. The structure of power controller of PHEV is specified as a PI with single input. Based on an enhancement of stabilizing performance and robust stability margin against system uncertainties, the PI parameters optimization problem can be formulated. By particle swarm optimization (PSO) [19], the PI parameters are automatically tuned without the difficulty of weighting functions selection in the mixed

H_2/H_∞ control. Simulation results confirm that the proposed specified structure mixed H_2/H_∞ controller is much superior to the conventional controller in terms of disturbance attenuation performance and robustness against various uncertainties.

This paper is organized as follows. First, the study system and modeling are presented in Section 2. Next, Section 3 describes the proposed specified structure mixed H_2/H_∞ controller design. Subsequently, Section 4 demonstrates simulation results. Finally, conclusion is given in Section 5.

2. **Study System and Modeling.** A two-area interconnected power system [5] as illustrated in Figure 1 is used for the study of smart grid. Each area consists of wind farm (WF), thermal power plant (THP), LFC, PHEV and load. In area 1, the power capacities of WF, THP and load are 12038 MW, 33090 MW and 7090 MW, respectively. For area 2, the power capacities of WF, THP and load are 2530 MW, 5560 MW and 7090 MW, respectively. In area 1, there are 640000 PHEVs while there are 200000 PHEVs in area 2. For one PHEV, the rated power capacity is 5 kW. Accordingly, the total power capacities of PHEVs in areas 1 and 2 are 3200 MW and 1000 MW, respectively.

The local control center in each area sends the control signal via the smart meter to the PHEV. The intermittent wind power and random load changes cause the severe frequency fluctuation in both areas. Besides, the capacity of turbine (TB) and governor (GOV) of THP is inadequate for keeping the frequency fluctuation in an acceptable range. To deal with this problem, the PHEVs installed in both areas are applied to cooperate with TB and GOV of THP for compensation of the sudden unbalance of power generation and load, because the dynamic response of PHEV is faster than that of TB and GOV of THP. Then, the operational tasks are selected according to the speed response as follows. The PHEV is in charge of suppressing the peak value of frequency deviation rapidly against the abrupt load change. Subsequently, the GOV and TB of THP are utilized for eliminating the stead-state error of frequency deviation. Consequently, the TB and GOV models are neglected in the control design of PHEV.

The linearized model of two-area interconnected power system [5] is demonstrated in Figure 2. In each area, the generator and frequency sensitive load are represented by the

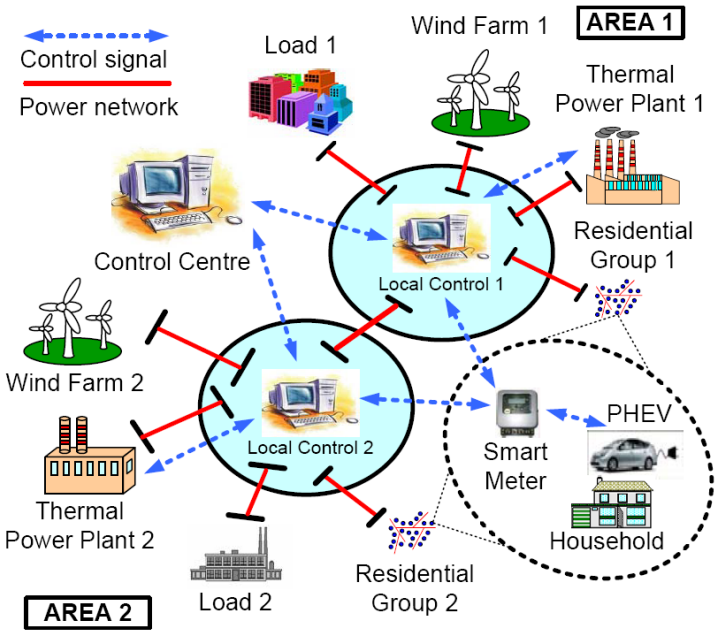

FIGURE 1. Two-area interconnected power systems

1st-order transfer function with the inertia constant M and damping coefficient D. The PHEV is represented by the 1st-order transfer function with gain K_{PHEVi}, $i = 1, 2$ and time constant T_P in series with the PI-based bidirectional power charging controller with gain K_{Pi} and time constant K_{Ii}. The wind power and load change are modeled by the random power sources ΔP_W and ΔP_L, respectively. The LFC in each area is based on the tie-line bias control. The frequency controller in each area is the 1st-order transfer function with time constant T_{ACEi} with the area control error (ACE_i) as an input signal. Note that $ACE_1 = f_0 K_{system1} \Delta f_1 - \Delta P_{21}$ and $ACE_2 = f_0 K_{system2} \Delta f_2 - a_{21} \Delta P_{21}$ where, $K_{system1}$ and $K_{system2}$ are the system constants of areas 1 and 2, respectively, f_0 is the normal system frequency, a_{21} is the area capacity ratio, ΔP_{21} is the deviation of tie-line power from area 2 to area 1, and T is the synchronizing power coefficient. The ACE signal from frequency controller is sent to PHEV via the smart meter. System parameters are given in Table 1.

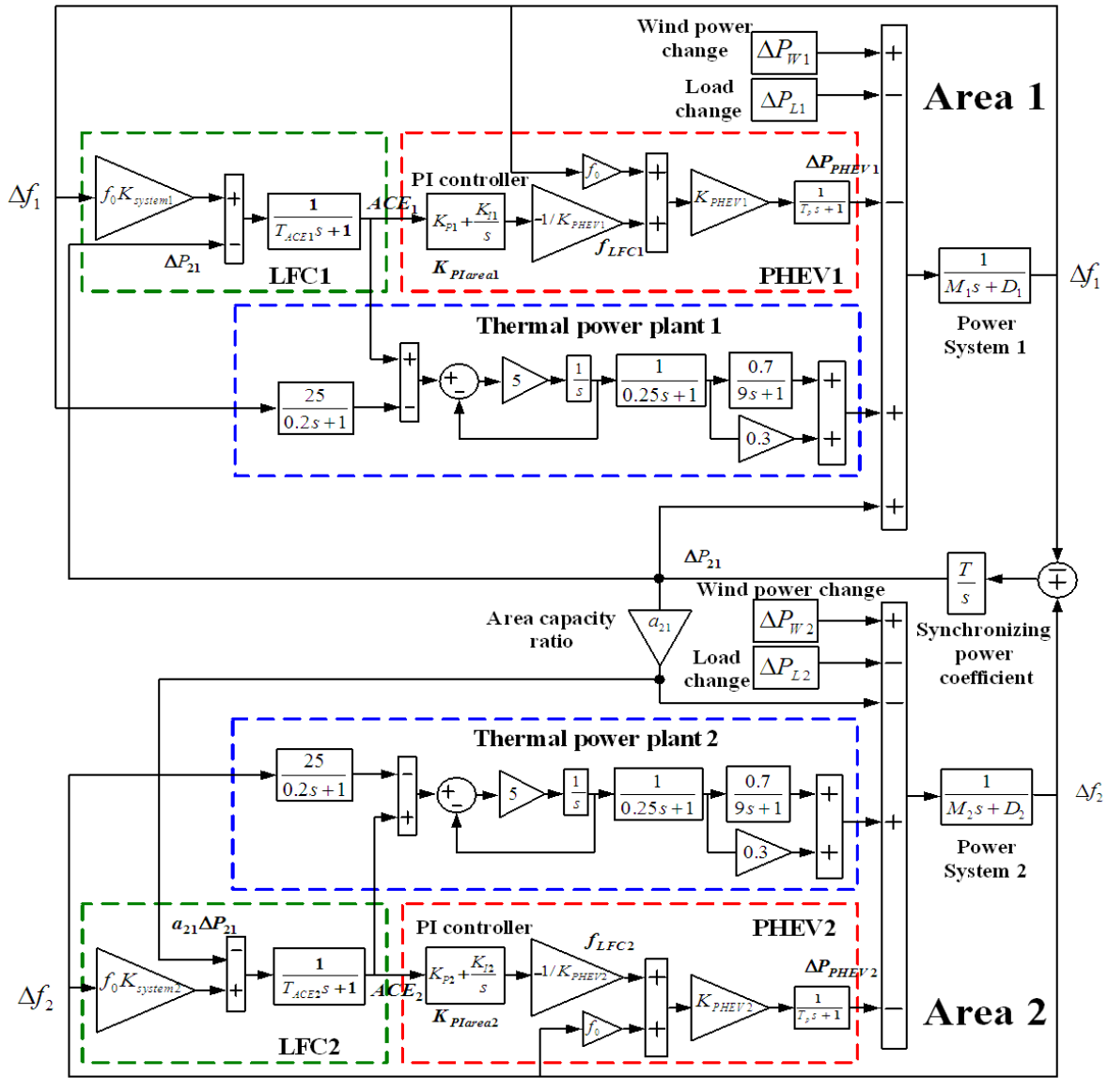

FIGURE 2. Linearized model of two-area interconnected system

TABLE 1. System parameters

Parameters	Area 1	Area 2
Reference frequency f_0 (Hz)	50	50
Inertia constant M (s)	9	9
Frequency characteristic of load except PHEV D (pu)	2	2
ACE calculation time constant T_{ACE} (s)	10	10
Frequency bias factor K_{system} (%MW/Hz)	10	10
Frequency characteristic per PHEV (kW/Hz)	2.5	2.5
Number of PHEV	640,000	200,000
Total frequency characteristic K_{PHEV} (MW/Hz)	1,600	500
Time constant of PHEV T_P (s)	1	1
Tie-line stiffness coefficient T (s)	5	
Area capacity ratio (a_{21})	0.17	

The linearized state equations of system without TB and GOV for design of PHEV controller in Figure 2 can be expressed as

$$\Delta\dot{\boldsymbol{X}} = \boldsymbol{A}\Delta\boldsymbol{X} + \boldsymbol{B}\Delta\boldsymbol{u} \tag{1}$$

$$\Delta\boldsymbol{Y} = \boldsymbol{C}\Delta\boldsymbol{X} \tag{2}$$

where $\boldsymbol{A}$ is the system matrix, $\boldsymbol{B}$ is the input matrix and $\boldsymbol{C}$ is the output matrix as follows.

$$A = \begin{bmatrix} \frac{-D_1}{M_1} & 0 & \frac{-1}{M_1} & \frac{1}{M_1} & 0 & 0 & 0 \\ \frac{f_0 K_{system1}}{T_{ACE1}} & \frac{-1}{T_{ACE1}} & 0 & \frac{-1}{T_{ACE1}} & 0 & 0 & 0 \\ K_{PHEV1} f_0 & 0 & -1 & 0 & 0 & 0 & 0 \\ -T & 0 & 0 & 0 & T & 0 & 0 \\ 0 & 0 & 0 & \frac{-a_{21}}{M_2} & \frac{-D_2}{M_2} & 0 & \frac{-1}{M_2} \\ 0 & 0 & 0 & \frac{-a_{21}}{T_{ACE2}} & \frac{f_0 K_{system2}}{T_{ACE2}} & \frac{-1}{T_{ACE2}} & 0 \\ 0 & 0 & 0 & 0 & K_{PHEV2} f_0 & 0 & -1 \end{bmatrix}$$

$$B = \begin{bmatrix} 0 & 0 \\ 0 & 0 \\ K_{PHEV1} & 0 \\ 0 & 0 \\ 0 & 0 \\ 0 & 0 \\ 0 & K_{PHEV2} \end{bmatrix} \quad C = \begin{bmatrix} 0 & 1 & 0 & 0 & 0 & 0 & 0 \\ 0 & 0 & 0 & 0 & 0 & 1 & 0 \end{bmatrix}$$

The PI controllers of PHEV in areas 1 and 2 are expressed by

$$K_{PIarea1}(s) = K_{P1} + \frac{K_{I1}}{s} \tag{3}$$

$$K_{PIarea2}(s) = K_{P2} + \frac{K_{I2}}{s} \tag{4}$$

where the state vector $\Delta\boldsymbol{X} = [\Delta f_1, ACE_1, \Delta P_{PHEV1}, \Delta P_{21}, \Delta f_2, ACE_2, \Delta P_{PHEV2}]^T$. Δf_1 and ΔP_{PHEV1} are the deviations of frequency and PHEV power in area 1, respectively. ACE_1 is the area control error in area 1. ΔP_{21} is the deviation of tie-line power flow from area 2 to area 1. Δf_2 and ΔP_{PHEV2} are the deviations of frequency and PHEV power in area 2, respectively. ACE_2 is the area control error in area 2. The output vector $\Delta\boldsymbol{Y} = [ACE_1 \ ACE_2]^T$, the control output signal $\Delta\boldsymbol{u} = [f_{LFC1}, f_{LFC2}]^T$. f_{LFC1} and f_{LFC2} are the LFC signals in areas 1 and 2, respectively. $K_{PIarea1}(s)$ and $K_{PIarea2}(s)$

are the designed PI controllers of PHEV in areas 1 and 2, respectively. K_{P1} and K_{P2} are proportional controller gains. K_{I1} and K_{I2} are integral controller gains. The system (1) is a multi-input multi-output (MIMO) system and referred to as the nominal plant. The PI parameters in (3) and (4) are optimized by the proposed method.

3. **Proposed Specified Structure Mixed H_2/H_∞ Control Design.** In the practical control application, multi-objectives such as disturbance attenuation, stability and reference tracking under model uncertainties and practical constraints are followed simultaneously. On the other hand, each robust control method is mainly useful to capture a set of special design specifications. For example, noise attenuation or regulation against random disturbances is more naturally expressed in Linear Quadratic Gaussian (LQG) terms (H_2 synthesis). Similarly, pure H_∞ synthesis is more useful for holding close loop stability and formulation of some uncertainties and practical control constraints. It is shown that combination of H_2 and H_∞ (mixed H_2/H_∞) control techniques gives a powerful multi-objectives design including both sets of the above objectives [12,13]. Nevertheless, the difficulty of selection of weighting functions in the mixed H_2/H_∞ control is an inevitable problem. Besides, the high-order controller which is not easy to implement in real systems, is obtained. To tackle these problems, the PI-based mixed H_2/H_∞ optimization is presented. The proposed design method is presented as follows.

3.1. **Mixed H_2/H_∞ control method.** To improve the robustness of PHEV controllers against unstructured system uncertainties, the inverse output multiplicative perturbation [20] is applied to represent system uncertainties such as variation of system parameters, wind power change and several loading conditions without exact mathematic representation. The control system with inverse output multiplicative perturbation and external disturbance is shown in Figure 3(a) where G is the nominal plant, K is the designed controller, $r(t)$ is the reference input, $e(t)$ is the error tracking, $d(t)$ is the external disturbance, $y(t)$ is the output of the system and Δ_M is the multiplicative uncertainty model.

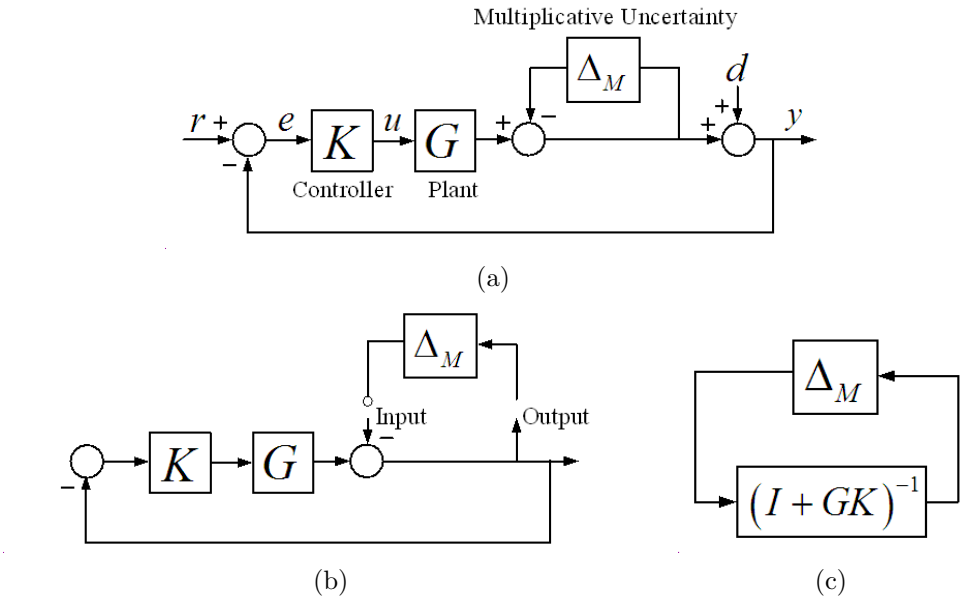

FIGURE 3. (a) Feedback system with inverse output multiplicative perturbation, (b) obtaining the transfer function from the uncertainty and (c) the system as seen by the uncertainty

Here the small gain theory is applied to formulate the optimization problem based on the feedback system in Figure 3(a). First, find the transfer function seen by the uncertainty block. The input and output of this block are shown at the indicated points in Figure 3(b), and its transfer function is $(I + GK)^{-1}$ as given in Figure 3(c). By the small gain theorem, if $(I + GK)^{-1}$ and Δ_M are stable, the closed loop system will be robustly stable if

$$\left\|\Delta_M \left(I + GK\right)^{-1}\right\|_\infty < 1 \tag{5}$$

where $\|\|_\infty$ is the infinite norm of the transfer function. Then,

$$\|\Delta_M\|_\infty < 1 \Big/ \left\|\left(I + GK\right)^{-1}\right\|_\infty \tag{6}$$

The right hand side of (6) implies the size of system uncertainties or the robust stability margin against system uncertainties. By minimizing $\|(I+GK)^{-1}\|_\infty$, the robust stability margin of the closed-loop system is maximum. This concept can be applied to design a robust controller when the following cost function J_∞ is minimized.

$$J_\infty = \left\|\left(I + GK\right)^{-1}\right\|_\infty \tag{7}$$

In many control systems, not only the robust stability against plant perturbation and external disturbances, but also the small tracking error is also important. The problem of minimizing the tracking error of a system in H_2 control can be defined as minimizing the cost function, called the integral of the square error

$$J_2 = \int_0^\infty e^T(t)e(t)dt = \|E(s)\|_2^2 \tag{8}$$

where $e(t) = r(t) - y(t)$ is the error signal and $\|\|_2$ is the 2-norm of transfer function. $E(s)$ which is the Laplace transformation of $e(t)$ can be obtained when taking $\Delta_M = 0$ and $d(t) = 0$ as

$$E(s) = \left(I + G(s)K(s)\right)^{-1} R(s) \tag{9}$$

where $R(s)$ is the Laplace transformation of $r(t)$.

By combining (7) and (8), the multi-objective PI-based mixed H_2/H_∞ optimization can be formulated as

$$\begin{aligned} &\text{Minimize } J_2 + J_\infty \\ &\text{Subject to } 0.0001 < K_{Pi} < 5, \\ &\qquad\qquad 0.0001 < K_{Ii} < 5, \quad i = 1, 2 \end{aligned} \tag{10}$$

The novel contribution of the proposed optimization can be described as follows.

(1) Without trial and error, the PI parameters of PHEV controller can be automatically optimized by PSO.

(2) In the proposed optimization, the difficulty of the selection of weighting functions as in the conventional mixed H_2/H_∞ control can be eliminated.

(3) The proposed optimization guarantees the designed controller with high performance and robustness against system uncertainties.

This problem is automatically solved by PSO.

3.2. **PSO algorithm.** The PSO was discovered through simulation of a simplified social model, where each population is called a swarm. In PSO, multiple solutions collaborate simultaneously. Each candidate, called a particle, flies through problem space to look for the optimal position, similar to food searching of bird swarm. A particle adapts its position based on its own knowledge, and knowledge of neighboring particles. The algorithm is

initialized with a population of random particles. It searches for the optimal solution by updating particles in generations. Figure 4 depicts the flowchart of PSO algorithm.

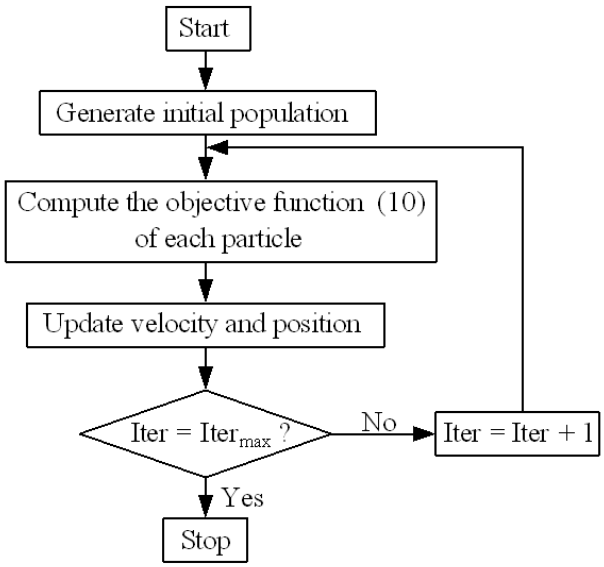

FIGURE 4. Flowchart of PSO algorithm

The PSO algorithm [19] is briefly explained as follows:

(1) Specify the parameters of PSO. Initialize a population of the particles with random positions and velocities.

(2) Evaluate the objective function in (10) for each particle.

(3) Compare the fitness value of each particle with its best position for particle (*pbest*). The best fitness value among all *pbests* is the best position of all particles in the group (*gbest*).

(4) Update the velocity v_i and position of particle x_i by

$$v_{i+1} = w.v_i + c_1.rand_1.(pbest - x_i) + c_2.rand_2.(gbest - x_i) \tag{11}$$

$$x_{i+1} = x_i + v_{i+1} \tag{12}$$

$$w = w_{\max} - \frac{w_{\max} - w_{\min}}{iter_{\max}} iter \tag{13}$$

where c_1 and c_2 are the cognitive and social acceleration factors, respectively. $rand_1$ and $rand_2$ are the random numbers of range (0,1). w is the inertia weight factor. $w_{\min}$ and $w_{\max}$ are the minimum and maximum of inertia weight factors, respectively. $iter$ and $iter_{\max}$ are the iteration count and maximum iteration, respectively.

(5) When the maximum number of iterations is arrived, stop the process. Otherwise go to step 2.

The motivation of the practical use of the theoretic results obtained can be summarized as follows.

(1) When the penetration of wind farms to interconnected power system increases considerably, it may cause the severe frequency fluctuation. To overcome this problem, the proposed robust power controller of PHEV can be applied.

(2) When the frequency control capability of the generators is not sufficient, especially in the night time when the electricity price is low, the PHEVs which are generally plugged into the outlets, can contribute to frequency control. By the proposed power controller of PHEV, the frequency fluctuation can be alleviated.

(3) The proposed power controller of PHEV can be coordinated with the conventional frequency controller. The PHEV can be used to reduce the transient frequency fluctuation when the sudden change in wind power occurs. Subsequently, the conventional frequency controller gets rid of the steady-state error of the frequency fluctuation.

(4) Since the PI-based power controller of PHEV has a practical structure, it can be easily implemented in the real system.

(5) Without trial and error or designer's experiences, the PI control parameters of the bidirectional power controller can be obtained by the proposed optimization technique.

(6) The controller with high stabilizing effect under various disturbances and high robustness against system uncertainties such as variation of system parameters and several operating conditions, can be achieved by the proposed method.

4. **Simulation Results.** The conditions imposed to develop the main results and some computation issues can be given as follows.

(1) Since the small disturbances, i.e., load change and wind power change are considered in this study, the system model can be linearized around a stable operating point [21]. The simulation study can be carried out in the linearized system.

(2) Since the converter equipped with PHEV has a very fast response, they can be represented by the 1st-order transfer function with time constant T_P [5].

(3) The wind power and load change are represented by a random active power source for simplicity [22].

(4) The simulation study is performed by MATLAB and Simulink [23].

The constant parameters of PSO are set as follows; PSO sizes = 50, maximum iterations = 100, $c_1 = 2$, $c_2 = 2$, $w_{\min} = 0.4$ and $w_{\max} = 0.9$. After solving the optimization problem (10), the convergence curve of the objective function can be delineated in Figure 5.

As a result, the optimized PI parameters of PHEV controllers are

$$K_{PHEV1}(s) = 3.535 + \frac{0.812}{s} \tag{14}$$

$$K_{PHEV2}(s) = 1.912 + \frac{0.638}{s} \tag{15}$$

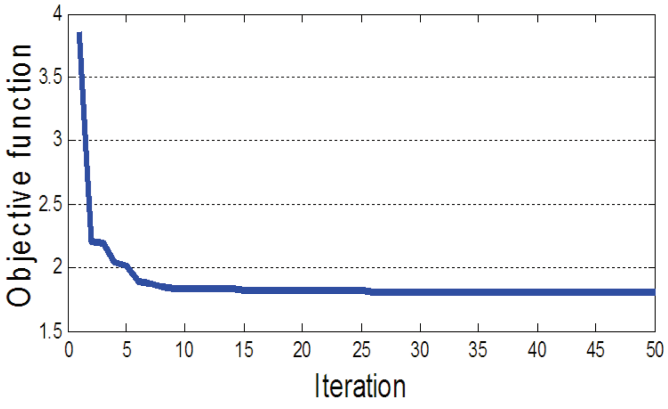

FIGURE 5. Convergence curve

Here, the proposed robust controllers are compared with the conventional controllers designed by minimizing the integral absolute error (IAE) of frequency deviation as

$$\begin{aligned} &\text{Minimize} \int_0^{t_f} (|\Delta f_1(t)| + |\Delta f_2(t)|)dt \\ &\text{Subject to } 0.0001 < K_{Pi} < 5, \\ &\qquad\qquad 0.0001 < K_{Ii} < 5, \quad i = 1, 2 \end{aligned} \tag{16}$$

where t_f is the final time of simulation. The optimization problem (16) is also solved by PSO.

Simulation studies are carried out by three case studies as follows.

Case 1 **Step load change**

It is assumed that the 0.1 puMW step load is applied to area 1. Figure 6 shows the frequency deviation of area 1 in case of the linearized system without TB and GOV. Without PHEV, the frequency deviation suddenly decreases and reaches the steady-state value. Note that, since TB and GOV are not included in the system, the steady-state error cannot be eliminated to be zero. On the other hand, in case of PHEV with IAE controller or proposed controller, the first peak frequency is considerably reduced by the stabilizing effect of PHEV. The remaining steady-state error is less than that in case of without PHEV.

Next, simulation results when TB and GOV are included in the system, are depicted in Figure 7. Without PHEV, the steady-state error of frequency deviation is gradually eliminated to be zero after the sudden drop of system frequency. With PHEV, after the transient frequency error is considerably diminished by the PHEV, the TB and GOV continuously eliminate the steady-state error completely. These results confirm the coordinated control between PHEV and TB-GOV that the PHEV reduces the transient frequency fluctuation while the TB and GOV get rid of the steady-state error to be zero.

Case 2 **Wind power and random load change**

It is assumed that the power systems with TB and GOV are subject to the wind power fluctuation and random load change as shown in Figures 8 and 9, respectively. Note that the maximum fluctuation of wind power is 3200 MW which is very severe. The frequency deviations of areas 1 and 2 and the tie-line power deviation are shown in Figures 10-12, respectively. The stabilizing effect of PHEV with proposed method is better than that of the PHEV with IAE method. The PHEV with proposed method is more robust against

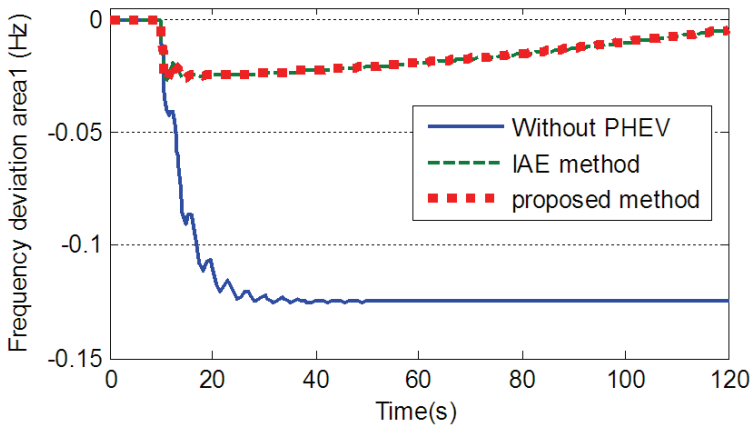

FIGURE 6. Frequency deviation of area 1 (without TB and GOV)

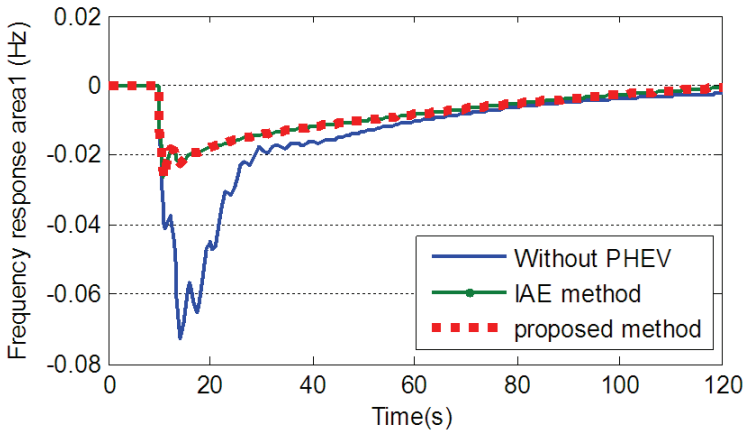

FIGURE 7. Frequency deviation of area 1 (with TB and GOV)

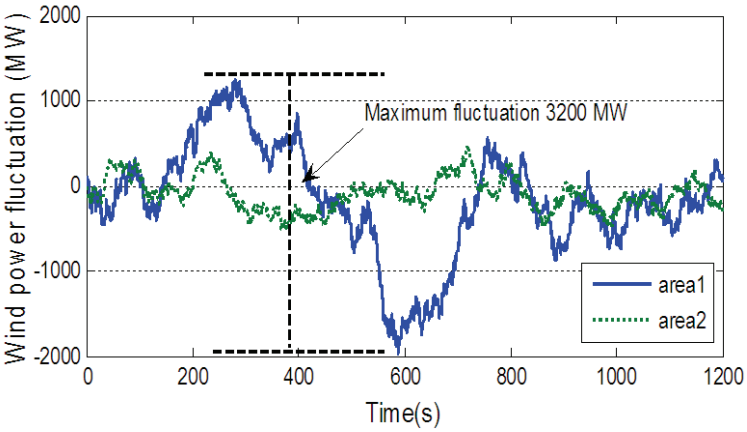

FIGURE 8. Power output from wind farms in both areas

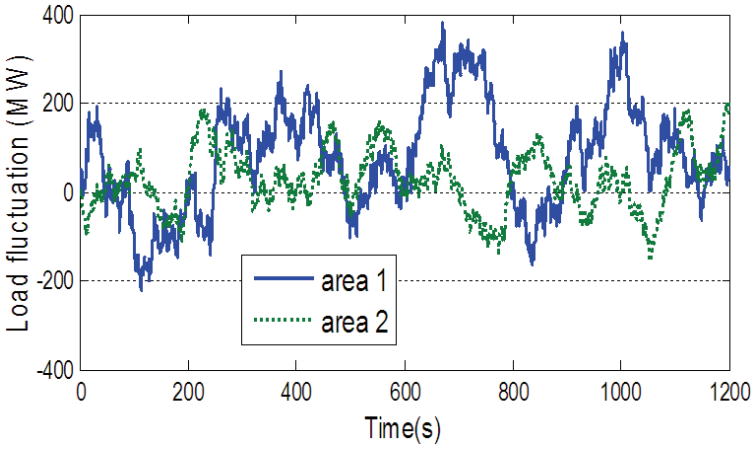

FIGURE 9. Load change in both areas

random wind and load power than the PHEV with IAE method. Figures 13 and 14 depict the bidirectional power transfer of PHEV in areas 1 and 2, respectively.

Case 3 **Changed system parameters**

In this case, the system is subject to the same wind power fluctuation and load change as in Figures 8 and 9, respectively. Figures 15, 16 and 17 show the variation of absolute

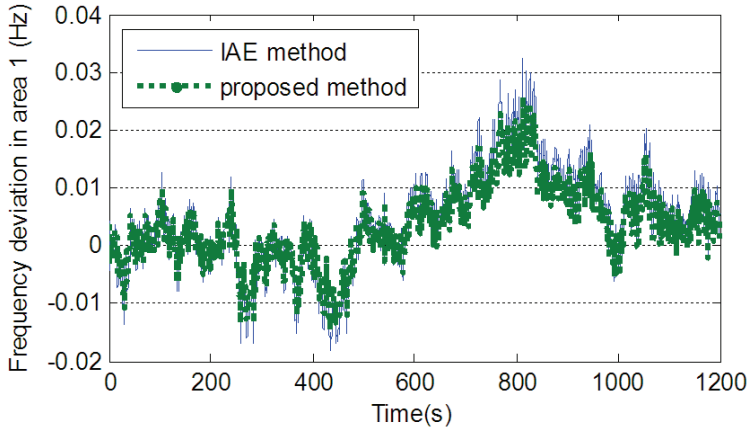

FIGURE 10. Frequency deviation in area 1

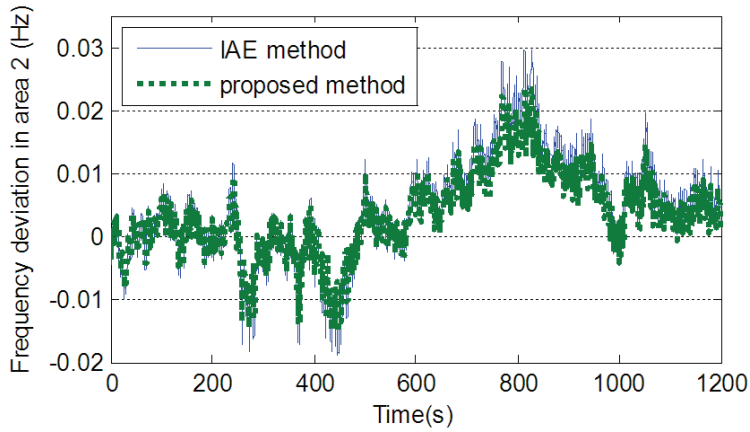

FIGURE 11. Frequency deviation in area 2

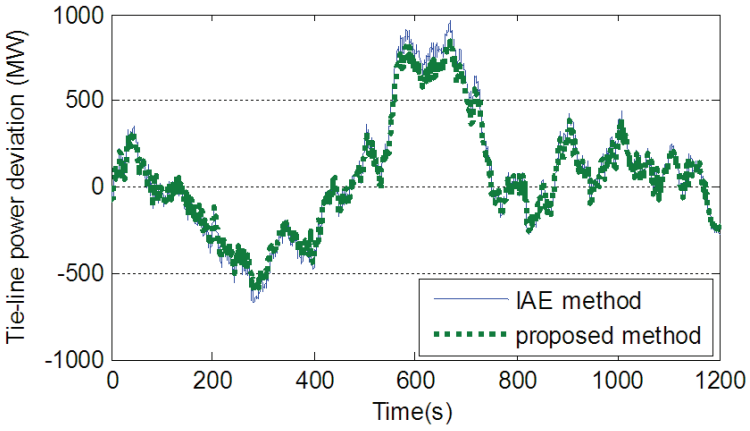

FIGURE 12. Tie-line power deviation

value of the maximum frequency deviation in area 1, the maximum frequency deviation of area 2 and the maximum tie-line power deviation, respectively, when the inertia constants (M_1 and M_2) and damping coefficients (D_1 and D_2) in both areas are varied from 0 to 40% of the normal values. Clearly, the PHEV with IAE controller is very sensitive to the parameters variation. The variation of frequency and tie-line power deviations in case of PHEV with IAE controller is higher than that in case of PHEV with proposed controller.

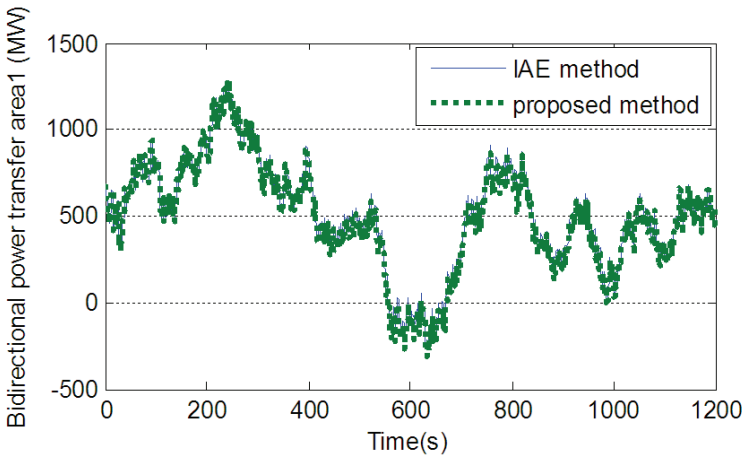

FIGURE 13. Bidirectional power transfer of PHEV area 1

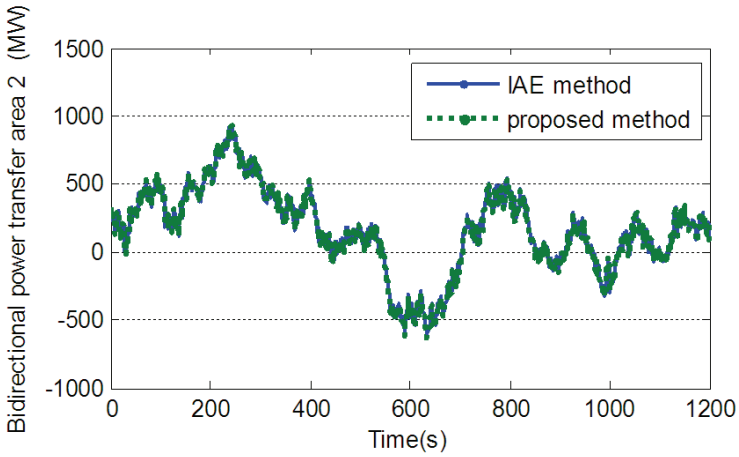

FIGURE 14. Bidirectional power transfer of PHEV area 2

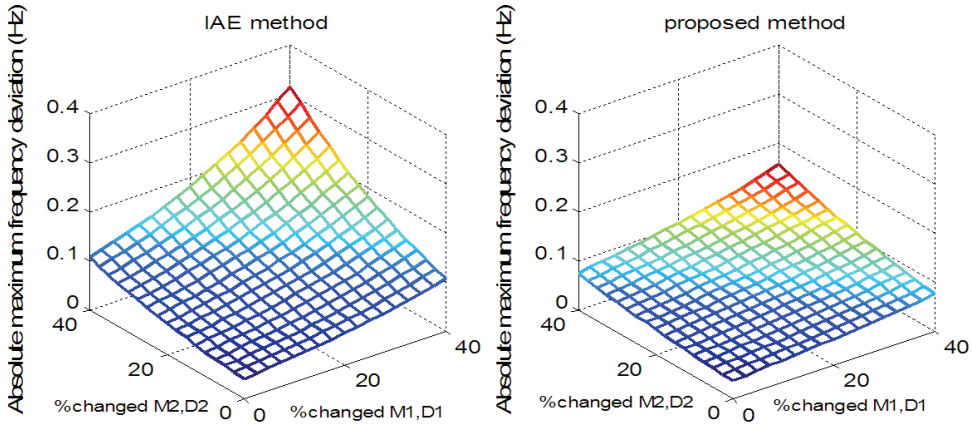

FIGURE 15. Variation of absolute value of the maximum frequency deviation of area 1

This implies that the proposed controller is more robust against system parameters variation than the PHEV with IAE controller.

Figures 18-20 show the frequency deviation of area 1, frequency deviation of area 2 and tie-line power deviation, respectively when M and D in both areas are increased by 40% from the normal values. Clearly, the PHEV with IAE controller is sensitive to the

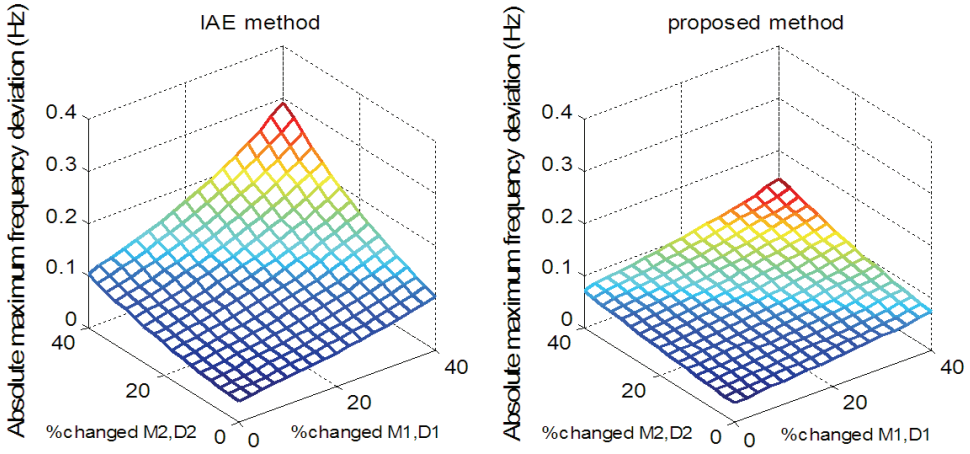

FIGURE 16. Variation of absolute value of the maximum frequency deviation of area 2

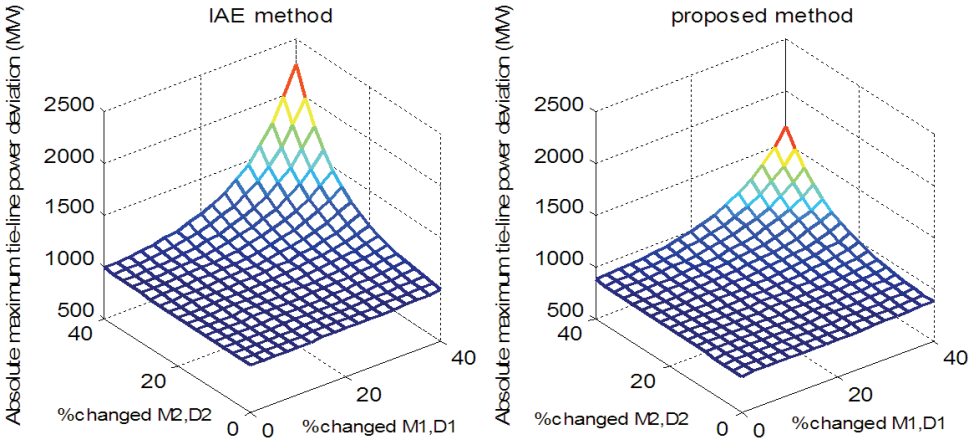

FIGURE 17. Variation of absolute value of the maximum tie-line power deviation

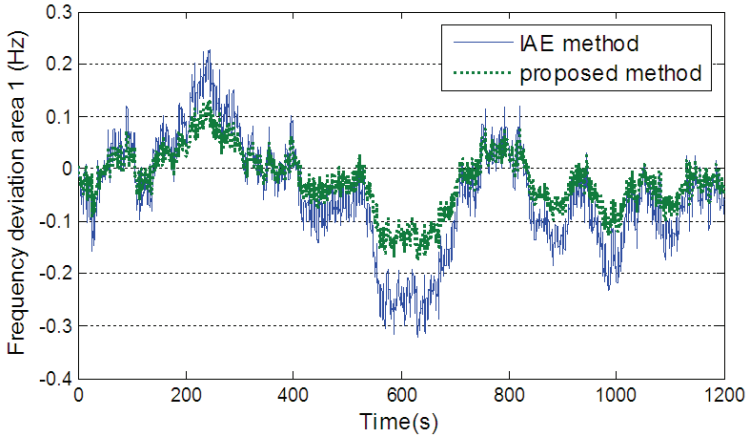

FIGURE 18. Frequency deviation of area 1 (40% increase in M and D)

parameters variation. Its control effect is considerably deteriorated. On the contrary, the PHEV with proposed controller can tolerate this situation. It can damp the frequency and tie-line power fluctuation robustly. The PHEV with proposed controller provides better damping effect than the PHEV with IAE controller. This is due to the higher power

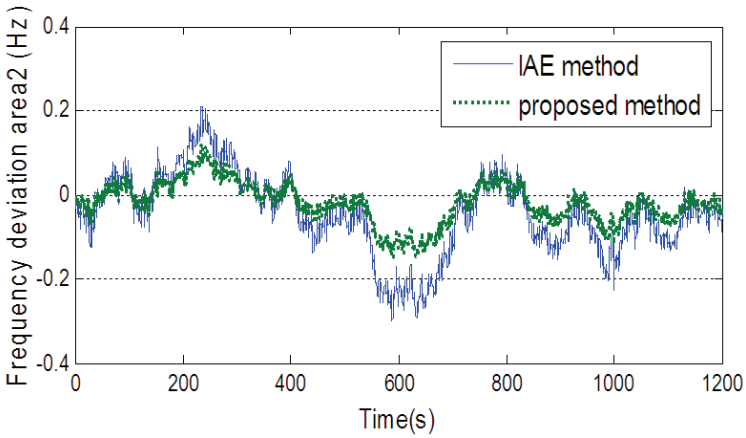

FIGURE 19. Frequency deviation of area 2 (40% increase in M and D)

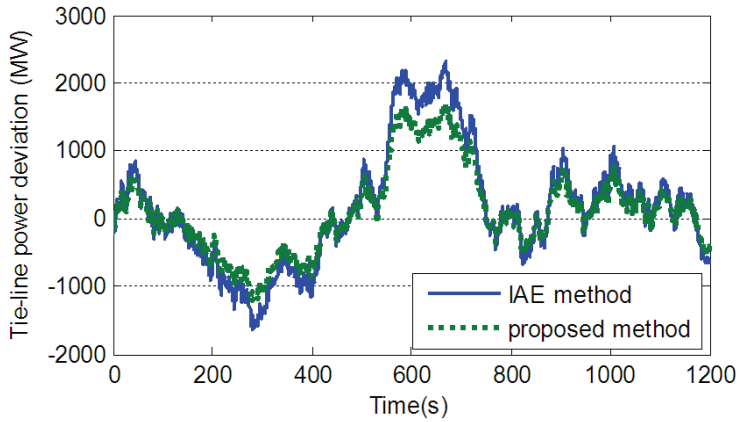

FIGURE 20. Tie-line power deivation (40% increase in M and D)

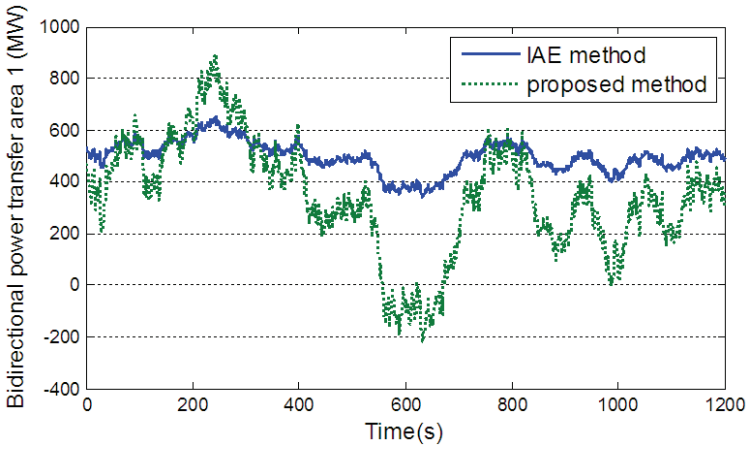

FIGURE 21. Bidirectional power transfer of PHEV area 1 (40% increase in M and D)

exchange of PHEV with proposed controller and the power systems as shown in Figures 21 and 22. These results confirm that the robustness and stabilizing effect of PHEV with proposed controller are much superior to those of the PHEV with IAE controller.

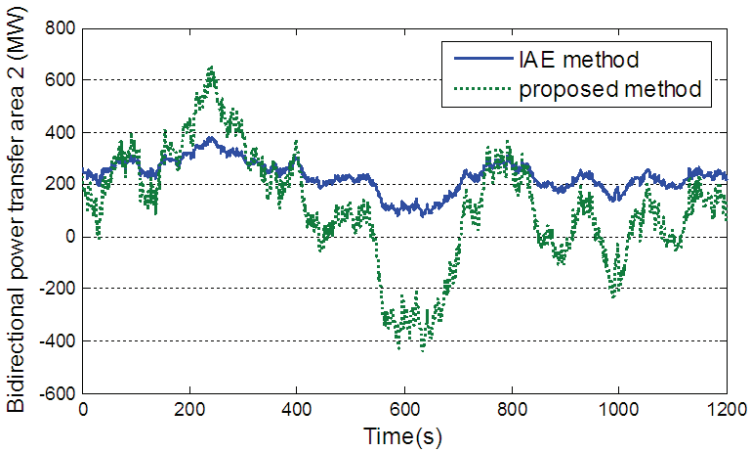

FIGURE 22. Bidirectional power transfer of PHEV area 2 (40% increase in M and D)

5. **Conclusion.** The new specified structure mixed H_2/H_∞ control has been proposed to design a bidirectional power charging controller of PHEV for stabilization of frequency fluctuation in the smart grid with wind farms. Without exact mathematical expressions, system uncertainties have been represented by the inverse input multiplicative model. To achieve the high performance and robustness, the optimal PI control parameters of PHEV controller are automatically tuned by PSO without the selection of weighting functions. Simulation results in the two-area interconnected power system with wind farms confirm the superior robustness and stabilizing effect of the proposed PHEV against system parameters variation, various wind power generations and load changes in comparison with the conventional PHEV controller.

Acknowledgment. This work was supported by the King Mongkut's Institute of Technology Ladkrabang Research Fund.

REFERENCES

[1] Smart grid – Putting it all together ... A 2010 reprint journal from PES, *IEEE Power & Energy Magazine*, 2010.
[2] A. Yokoyama, Smarter grid II, *IEEJ Journal*, vol.30, no.3, pp.163-167, 2010.
[3] T. Ackermann, *Wind Power in Power Systems*, Wiley, 2005.
[4] M. Takagi, H. Yamamoto, K. Yamaji, K. Okano, R. Hiwatari and T. Ikeya, Load frequency control method by charge control for plug-in hybrid electric vehicles with LFC signal, *IEEJ Transactions on Power and Energy*, vol.129, no.11, pp.1342-1348, 2009.
[5] M. Takagi, K. Yamaji and H. Yamamoto, Power system stabilization by charging power management of plug-in hybrid electric vehicles with LFC signal, *Proc. of IEEE Vehicle Power and Propulsion Conf.*, pp.822-826, 2009.
[6] Y. Ota, H. Taniguchi, T. Nakajima, K. M. Liyanage, K. Shimizu, T. Masuta, J. Baba and A. Yokoyama, Effect of autonomous distributed vehicle-to-grid (V2G) on power system frequency control, *Proc. of International Conference Industrial and Information System*, pp.481-485, 2010.
[7] Y. Ota, H. Taniguchi, T. Nakajima, K. M. Liyanage, K. Shimizu, T. Masuta, J. Baba and A. Yokoyama, Effect of autonomous distributed vehicle-to-grid (V2G) on power system frequency control effect of smart storage in ubiquitous power grid on frequency control, *IEEJ Transactions on Power and Energy*, vol.131, no.1, pp.94-100, 2011.
[8] Y. Ota, H. Taniguchi, T. Nakajima, K. M. Liyanage, K. Shimizu, T. Masuta, J. Baba and A. Yokoyama, Autonomous distributed vehicle-to-grid for ubiquitous power grid and its effect as a spinning reserve, *Proc. of the 16th International Conf. on Electrical Engineering*, 2011.

[9] C.-Y. Chen and G. T.-C. Chiu, H_∞ robust controller design of media advance systems with time domain specifications, *International Journal of Innovative Computing, Information and Control*, vol.4, no.4, pp.813-828, 2008.

[10] M. S. Mahmoud, Y. Shi and F. M. Al-Sunni, Robust H_2 output feedback control for a class of time-delay systems, *International Journal of Innovative Computing, Information and Control*, vol.4, no.12, pp.3247-3257, 2008.

[11] P. Pannil, K. Tirasesth, P. Ukakimaporn and T. Trisuwannawat, Derivative state constrained optimal H_2 control for unstable systems, *International Journal of Innovative Computing, Information and Control*, vol.5, no.10(B), pp.3541-3552, 2009.

[12] P. P. Khargonekar and M. A. Rotea, Mixed H_2/H_∞ control: A convex optimization approach, *IEEE Transactions on Automatic Control*, vol.36, no.7, pp.824-837, 1991.

[13] C. W. Scherer, Multi-objective H_2/H_∞ control, *IEEE Transactions on Automatic Control*, vol.40, no.2, pp.1054-1062, 1995.

[14] F. Jamshidi, M. G. Moghadam and M. T. H. Behesht, Synthesis of a logic-based switching H_2/H_∞ controller: An intelligent supervisor approach, *ICIC Express Letters*, vol.4, no.1, pp.7-12, 2010.

[15] M. M. Al-Harthi, Robust AVR design based on mixed H_2/H_∞ pole placement using linear matrix inequality (LMI), *ICIC Express Letters*, vol.4, no.3, pp.963-971, 2010.

[16] H. Shayeghi, A. Jalili and H. A. Shayanfar, A robust mixed H_2/H_∞ based LFC of a deregulated power system including SMES, *Energy Conversion and Management*, vol.49, no.10, pp.2656-2668, 2008.

[17] M. M. Farsangi, Y. H. Song and M. Tan, Multi-objective design of damping controllers of FACTS devices via mixed H_2/H_∞ with regional pole placement, *International Journal of Electrical Power and Energy Systems*, vol.25, no.5, pp.339-346, 2003.

[18] H. Bevrani, Y. Mitani and K. Tsuji, Robust decentralized AGC in a restructured power system, *Energy Conversion and Management*, vol.45, no.15-16, pp.2297-2312, 2004.

[19] J. Kennedy and R. C. Eberhart, Particle swarm optimization, *Proc. of IEEE International Conference on Neural Network*, pp.1942-1948, 1995.

[20] D. W. Gu, P. H. Petkov and M. M. Konstantinov, *Robust Control Design with MATLAB*, Springer, 2005.

[21] P. Kundur, *Power System Stability and Control*, McGrawhill, 1994.

[22] S. Vachirasricirikul, I. Ngamroo and S. Kaitwanidvilai, Application of electrolyzer system to enhance frequency stabilization effect of microturbine in a microgrid system, *International Journal of Hydrogen Energy*, vol.34, no.17, pp.7131-7142, 2009.

[23] *http://www.mathworks.com/*.